European Review for Medical and Pharmacological Sciences 2018; 22: 1700-1708

MicroRNA-520a-3p suppresses non-small-cell lung carcinoma by inhibition of High Mobility Group Box 1 (HMGB1)

X. LV[1], L. YAO[2], Y.-Q. NIE[1], X.-Y. XU[1]

[1]Department of Respiratory, Linyi People's Hospital, Linyi, China
[2]Department of General, Linyi People's Hospital, Linyi, China

Abstract. – OBJECTIVE: Currently, pathogenesis of non-small cell lung carcinoma (NSCLC) is still unknown and the treatment is far from ideal. Therefore, we investigated the effect of inhibiting microRNA-520a-3p in NSCLC cells.

MATERIALS AND METHODS: NCI-H157 cells were treated with microRNA-520a-3p analogs for 48 h, or microRNA-520a-3p analogs and its inhibitor, for a total of 48 h. Many tests were performed, including MTT, flow cytometry, wound healing assay and transwell assay. The tumor model was established, and HMGB1 mRNA was detected by RT-PCR. Protein levels of HMGB1, MMP-2, MMP-9, Bcl-2, Bax, and Caspase-3 were assessed by Western Blot.

RESULTS: microRNA-520a-3p could significantly inhibit the proliferation, migration and invasion of NCI-H157 cells, inducing their apoptosis. microRNA-520a-3p inhibited tumor growth and decreased the mRNA and protein levels of HMGB1. Additionally, it decreased the Bcl-2/Bax ratio, MMP-2 and MMP-9 expression, and increased caspase-3 expression.

CONCLUSIONS: microRNA-520a-3p exhibited an effective inhibition on NCI-H157 tumor growth likely by inhibiting HMGB1 expression.

Key Words
Non-small-cell lung carcinoma, microRNA-520a-3p, HMGB1, Tumorigenesis.

Abbreviations

BSA, Bovine Serum Albumin; Bcl-2, B-cell lymphoma-2; Bax, Bcl-2 Associated X Protein; ECL, Enhanced chemiluminescence; HMGB1, High mobility group box 1 protein; MTT, Methyl thiazolyl tetrazolium; MMPs, Matrix metalloproteinases; MMP-2, matrix metalloproteinase-2; MMP-9, matrix metalloproteinase-9; NSCLC, Non-small cell lung carcinoma; RT-PCR, Real time reverse transcription-polymerase chain reaction; PVDF, Polyvinylidene difluoride; RAGE, receptor for advanced glycationend product; MAPK, mitogen-activated protein kinase; SCLC, Small cell lung cancer; SNK, Student-Newman-Keuls; SPF, Specific pathogen Free; TBS-T, Tris-buffered saline and Tween 20.

Introduction

Lung cancer is still the most common cause of cancer death in the world despite recent progresses in diagnosis and therapies[1]. According to 2012 WHO data, lung cancer constitutes 13% of cancer incidence and is responsible for 19.4% of cancer mortality. Out of all lung cancer cases, non-small cell lung carcinoma (NSCLC), is consisting of three subtypes, adenocarcinoma, squamous cell carcinoma and large cell carcinoma, which accounts for 85% of all lung cancer cases[2,3]. Despite high rates of mortality and morbidity, the past decade has witnessed much progress in pathological classification and staging, early diagnosis with novel biological markers, and effective therapies for NSCLC[4,5].

NSCLC is traditionally diagnosed by CT scans or X-ray followed by tissue biopsies[6], while novel methods have been proposed based on close relations between cancer development and miRNA amount. Dysregulation of miRNAs has been found in many different cancers and it has been demonstrated that they play critical roles in cancer development. Under pathological conditions, miRNAs are often released from tissues into the circulation, and the miRNA profiles in biofluids (such as plasma and sputum) may be an accurate non-invasive indicator of discrete cancer types and stages[6-8].

MicroRNA-520 is a miRNA that has gained attention for its effect in limiting cancer cell growth. In 2014, Kaymaz et al[9] reported that microRNA-520p-5p acted as a mediator of anti-cancer effect of capsaicin. It was further demonstrated that microRNA-520p is capable of inhibiting proliferation, apoptosis and metastasis of cancer cells in both a non-small cell lung cancer and a Burkitt's lymphoma model[10,11].

As NSCLC is typically insensitive to chemical therapy, its treatment generally involves surgi-

Corresponding Author: Xinyi Xu, MD; e-mail: 13869996660@139.com

cal removal of the tumor, combined with neoadjuvant and adjuvant chemotherapies, as well as radiotherapies[5]. However, as our knowledge about the pathogenic mechanisms expands, more potential treatment targets have been identified[12]. High mobility group box 1 protein (HMGB1) is another target that has been proposed 10 years ago[13]. More recently, HMGB1 has been found to promote cell proliferation and invasion, and inhibit apoptosis, both in NSCLC and osteosarcomas, possibly by activating integrin alphavbeta3/FAK through TLR4/NF-kappaB signaling pathway[14,15]. The way HMGB1 promotes cancer growth is likely by downregulating p21 via ERK/c-Myc pathway and up-regulating matrix metalloproteinases (MMPs)[16]. Furthermore, HMGB1 has been reported to be regulated by a number of miRNAs, including miRNA-218 and miRNA-325-3p, which limit tumor growth by directly targeting HMGB1[17,18].

NCI-H157 cells are commonly used in *in vitro* NSCLC model[19]. In this study, we examined the effect of microRNA-520-3p on the NCI-H157 cells, and determined the relationship between this effect and HMGB1 expression. Here we report that microRNA-520a-3p effectively inhibits NCI-H157 cell proliferation, migration and invasion, and induces its apoptosis. When transplanted into nude mice NCI-H157 cells treated with microRNA-520-3p limited tumor growth, and decreased HMGB1, MMP-2 and MMP-9 expression. In summary, microRNA-520-3p is capable of effectively controlling NSCLC cell growth by suppressing HMGB1, and may provide a direction towards a novel HMGB1-targeted treatment of NSCLC.

Materials and Methods

Cell Culture

Human non-small-cell lung carcinoma cell line NCI-H157 (ATCC CRL-5802*, Manassas, VA, USA)* was grown on Roswell Park Memorial Institute 1640 (RPMI-1640) medium supplemented with 10% fetal bovine serum (FBS) (Gibco, Rockville, MD, USA) in a 37°C incubator with 5% CO_2. NCI-H157 cells in the logarithmic growth phase were treated with microRNA-520a-3p analog (Ambion, Waltham, MA, USA) for 24 h, and part of the cells were further treated with microRNA-520a-3p inhibitor (Dharmacon, Lafayette CO, USA) for 24 h. Doses of the microRNA-520a-3P analog and inhibitor were adjusted with the RT-PCR results, and the final concentration used was 30 nM of microRNA-520a-3P analog, and 25 nM of microRNA-520a-3P inhibitor. In *in vitro* experiments, cells were treated with the microRNA-520a-3P analog for 24 h, then half of the cells were continuously treated with the microRNA-520a-3P analog for more 24 h (Group Mimics), and the other cells were treated with the microRNA-520a-3P inhibitor for 24 h (Group M- Inhibitor).

MTT Assay

Cell viability was assayed by the MTT assay (Sigma-Aldrich, St. Louis, MO, USA). Three groups of NCI-H157 cells, Mimics, M-Inhibitor and Control (untreated) in the logarithmic growth phase were plated in 96-well plates. 200 µL MTT (5 mg/mL) were added to each well, and cells were incubated at 37°C for 4 h. 150 µL dimethyl sulfoxide (DMSO) (Sigma-Aldrich, St. Louis, MO, USA) was added to each well for 5 min, and absorbance was measured by Versamax microplate reader (Molecular Devices, Sunnyvale, CA, USA) at 490 nm.

Flow Cytometry Assay

Apoptosis was detected by Annexin V-fluorescein isothiocyanate (FITC) and propidium iodide (PI) double staining using the Annexin V Apoptosis Detection Kit (BD Biosciences, Franklin Lakes, NJ, USA). NCI-H157 cells of mimics, m-inhibitor and control groups in the logarithmic growth phase were grown in 6-well plates for 24 h. Next, cells were washed with phosphate-buffered saline (PBS), lifted by trypsin, resuspended in 100 µl binding buffer per well, and stained with Annexin V-FITC and PI for 15 min in the dark. 400 µl more binding buffer were added to each well, and cells were assayed by flow cytometry (CyAn ADP9, Beckman Coulter, Brea, CA, USA). The percentage of cells with apoptotic nuclei (% apoptosis) was calculated.

Wound Healing Assay

Three groups of NCI-H157 cells in the logarithmic growth phase were plated in 6-well plates. When they reached 80% confluence, the monolayers were scratched with a 10 µL pipet tip. Growth medium was removed, and the cells were washed with PBS. Cells were observed under a microscope (×100) (Olympus IX51, Olympus Corporation, Tokyo, Japan), and photos were taken at 0, 12 and 24 h after scratch.

Table I. Sequence of primers for microRNA-520a-3p.

RT primer	5'CTCAACTGGTGTCGTGGAGTCGGCAATTCAGTTGAGACAGTCCAAA3'
Forward primer	5'ACACTCCAGCTGGGAAAGTGCTTCCC3'
Reverse primer	5'CTCAACTGGTGTCGTGGA3'

Transwell Assay

8 μm pore size transwell chambers (Costar, Washington, WA, USA) were used to evaluate effect of microRNA-520a-3P on NCI-H1975 cell invasion. The upper chambers were coated with 1 mg/mL BD Matrigel Matrix (BD Biosciences, San Jose, CA, USA), and 200 μL cells in the Mimics, M-Inhibitor and Control groups suspended in fresh medium were added to the upper chamber for 24 h incubation. The invasion chambers were taken out, and surface cells and medium were removed with cotton swabs. Cells beneath the chamber membrane were fixed and stained with 0.1% crystal violet. For each group, 5 fields of view were randomly selected and counted under the microscope (×200, Olympus IX51, Olympus Corporation, Tokyo, Japan). The numbers were averaged for subsequent analysis.

Animal Experiment

30 healthy SPF-grade male BALB/c nude mice (Beijing CoLab., Bio-Technology Ltd., Beijing, China) were purchased (6 weeks of age, 18-22 g of body weight) and housed in an animal facility under 12 h light-dark cycles with a temperature between 20-24°C and *ad libitum* access to diet and water. The mice were acclimated for 1 week, and randomly divided in 3 groups (n=10), treated with NCI-H157 cells in three groups, respectively. NCI-H157 cells were digested and resuspended in PBS and injected into the right hip of the nude mice (1×10^7 cells per mouse). A series of physiological reactions were observed every 2 d, including stress, body weight change, skin lesion at the inoculation site, local response, time of induration appearance and tumor growth. The maximal diameters (d) of the tumors were measured at regular intervals. After 4 weeks, the mice were euthanized under aseptic conditions and tumor tissues were removed for subsequent analysis.

RT-PCR

Total RNA was extracted from the tumor tissue, and the concentration and purity were measured with a spectrophotometer. RT-PCR was performed with a TaKaRa two-step RT-PCR kit using 1 μg template RNA, random 6-mer primers in a 20 μL reactions. The RT reaction conditions were: 30 min at 37°C, 5 min at 83°C. PCR was performed in 10 μL reactions with the following reaction conditions: 2 min pre-denaturation at 94°C, 30 cycles of 30 s denaturation at 94°C, 30 s annealing at 56°C, and 90 s extension at 68°C, 12 min final extension at 68°C. PCR products were specified on 2.5% agarose gels containing 0.5 μg/mL of ethidium bromide and photographed under a UV transilluminator. Alpha Ease FC software (Miami, FL, USA) was used to analyze the relative light intensities. Parallel three experiments were performed. Primer sequences of HMGB1 and β-actin are listed in Table II.

Western Blot

Proteins were extracted and determined by Coomassie Brilliant Blue staining. Proteins of different groups (30 μg of protein per lane) were fractionated by sodium dodecyl sulphate-polyacrylamide gel electrophoresis (SDS-PAGE). The proteins were electro-transferred onto poly (polyvinylidene difluoride) (PVDF) membranes and were detected using dilutions of the primary antibodies. Anti-Bax, anti-Bcl-2, anti-caspase-3, anti- β-actin primary antibodies were purchased from Santa Cruz Biotechnology (Santa Cruz, CA, USA). Anti-MMP-2 and anti-MMP-9 primary antibodies were from Bioworld Technology, Inc. (St. Louis Park, MN, USA). Anti-mouse and anti-rabbit secondary antibodies were also from Santa Cruz Biotechnology (Santa Cruz, CA, USA). The bound antibodies were visualized using an enhanced chemiluminescence reagent (Millipore, Billerica, MA, USA) and images were analyzed with Quantity One gel analysis software (Bio-Rad, Hercules, CA, USA). Densitometric analyses of bands were adjusted with β-actin functioning as a loading control.

Table II. Primer sequences of tissue genes.

Genes	Primer sequence (5'-3')
HMGB1	F: GCGAGCATCCTGGCTTATC R: TTCAGCTTGGCAGCTTTCT
β-actin	F: CACAGCTGAGAGGGA AAT R:TCAGCA ATGCCTGGGTAC

Statistical Analysis

Statistical analysis was performed using the SPSS 19.0 program (IBM, Armonk, NY, USA). Comparisons between multiple groups were performed by one-way ANOVA, and comparisons between two groups were performed by the Student-Newman-Keuls (SNK) method. All data were presented as mean ± SD, and $p<0.05$ was considered statistically significant.

Results

Effect of microRNA-520a-3p on NCI-H157 Cell Proliferation and Apoptosis

As shown in Figure 1A, after treatment with microRNA-520a-3p analog, viability of NCI-H157 cells was 65.28 ± 5.11%, lower than the control cells ($p<0.01$), and in M-Inhibitor group the survival rate was significantly higher than the Mimics group ($p<0.05$). Flow cytometry results also showed clearly that the amount of apoptotic cells in the Mimics group was 23.5%, which is significantly higher than the Control groups. Whereas treated with M-inhibitor, the amount of apoptotic cells decreased to 11.2% (Figure 1B).

Effect of microRNA-520a-3p on NCI-H157 Cell Migration and Invasion

As shown in Figure 2A, wound healing assay showed that the Control group, Mimics group and M-Inhibitor group had scratch gaps of approximately the same width at 0 h. After 12 h, there were varying degrees of migration, then at 24 h, the width in the Mimics group was significantly larger than in the Control group ($p<0.05$), whereas the width in the M-Inhibitor group was significantly smaller than in the Mimics group ($p<0.05$). Transwell invasion assay results were consistent with the wound-healing assay. They also showed that the Mimics group had significantly decreased number of cells across the membrane than the Control group ($p<0.05$), and the M-Inhibitors group had significantly more cells across the membrane than the Mimics group ($p<0.05$, Figure 2B).

Effect of microRNA-520a-3p on NCI-H157 Tumor Xenograft Growth in Nude Mice

Intuitively, transplanted tumors were visible at 8, 10, and 16 days after inoculation in Control group, Mimics group and M-Inhibitors group, respectively. There were no dead mice in the process of tumorigenesis in all three groups. At the end of the experiment, the volume of transplanted tumors was significantly smaller than the Control group ($p<0.05$), whereas the volume of tumors in the M-Inhibitors group was significantly larger than the Mimics group ($p<0.05$). No distant metastasis was found in all three groups (Figures 3A and 3B). The whole tumors were separated from the nude mice and weighed. Tumor weight in Mimics group was significantly lower than that in Control group cells (3.25 *vs.* 1.8 g, $p<0.01$). However, after M-inhibitor treatment, tumor weight significantly increased (2.3 g, $p<0.05$, Figure 3C).

Effect of microRNA-520a-3p on HMGB1 Expression in NCI-H157 Tumor Xenograft Growth in Nude Mice

Expression of HMGB1 mRNA was measured by RT-PCR. As shown in Figure 4A, HMGB1 mRNA level in the Mimics group was significantly lower than the Control group (40% *vs.* 100%, of the control, $p<0.01$), and significantly lower than the

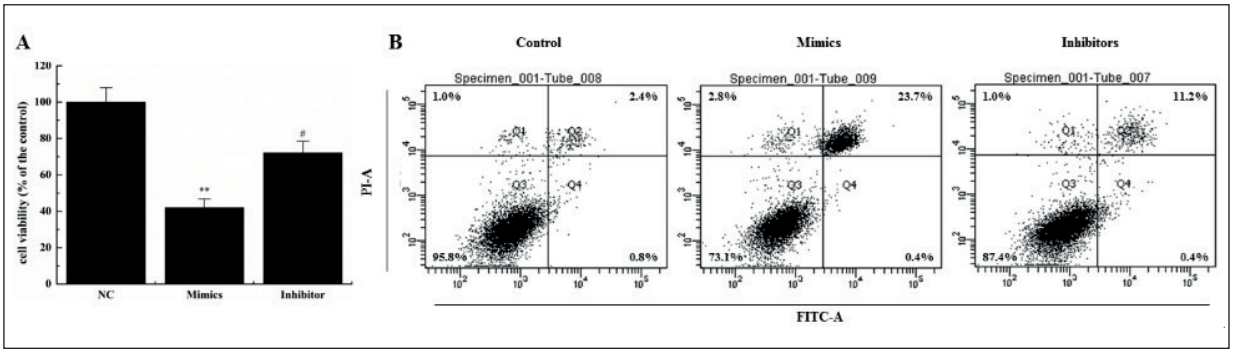

Figure 1. Effect of microRNA-520a-3p on NCI-H157 cell proliferation and apoptosis. **A**, Proliferation viability. **B**, Apoptosis detected by flow cytometry. Data were presented as mean ± SD. Compared with Control group, $^{**}p<0.01$; compared with Mimics group, $^{\#}p<0.01$.

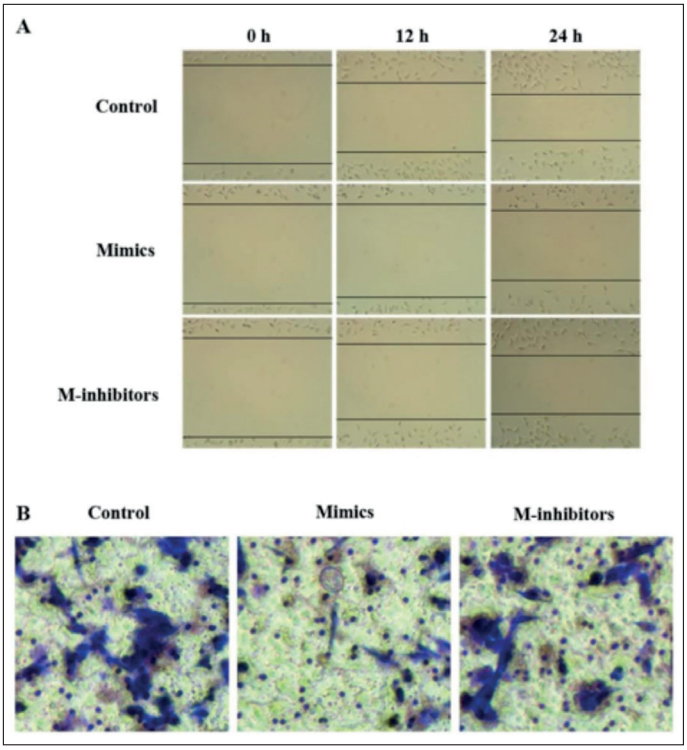

Figure 2. Effect of MicroRNA-520a-3p on NCI-H157 cellular migration and invasion activity by wound healing assay (**A**) and transwell invasion assay (**B**).

M-Inhibitors group (p<0.01, Figure 4A). Consistent with the RT-PCR results, the Western Blot also showed that HMGB1 protein level was downregulated after treating with microRNA-520a-3p analog, which was lower than the Control group (p<0.01). It can be seen from Figure 4B that M-inhibitors could improve the expression of HMGB1 protein (p<0.01). The level of HMGB1 protein in Control group, Mimic group and M-Inhibitor group was approximately 100%, 40% and 68%, respectively.

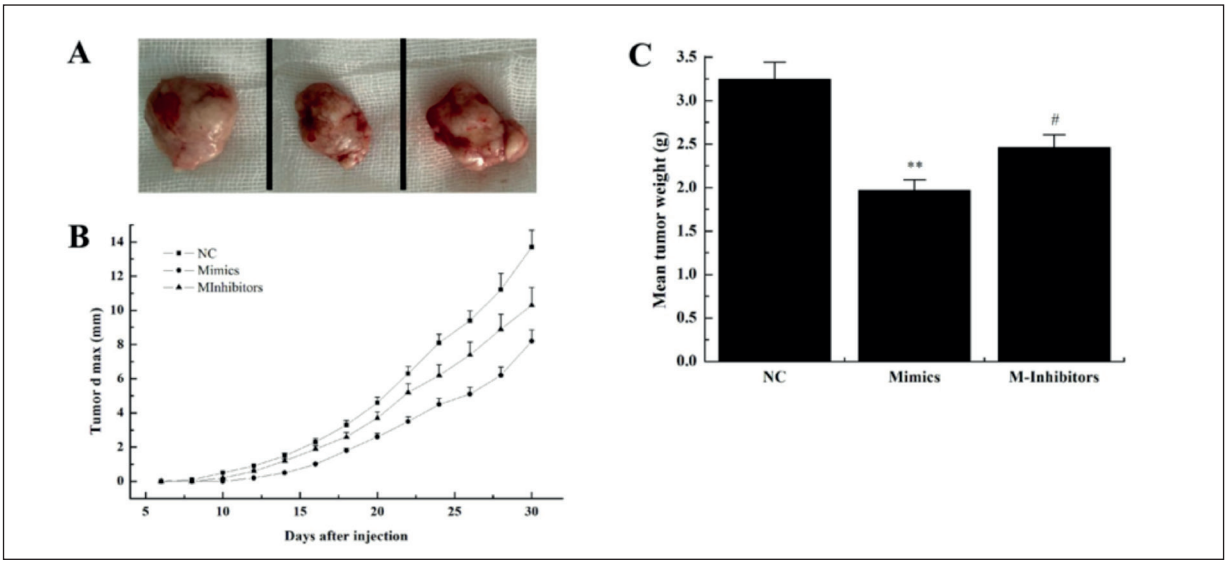

Figure 3. Tumorigenesis of NCI-H157 cells-bearing nude mice inoculated in Control group, Mimic group and M-Inhibitor group. **A**, Pictures of representative tumors. **B**, Growth curve of the largest tumor in each group. **C**, Average tumor weight. 1×107 cells were injected into the right hip of the nude mice. The tumor diameter and physiological condition were observed; the mice were sacrificed after 4 weeks. Data were presented as mean ± SD. *p<0.05; **p<0.01, compared with Control group; $^{\#}p$<0.05, compared with Mimics group.

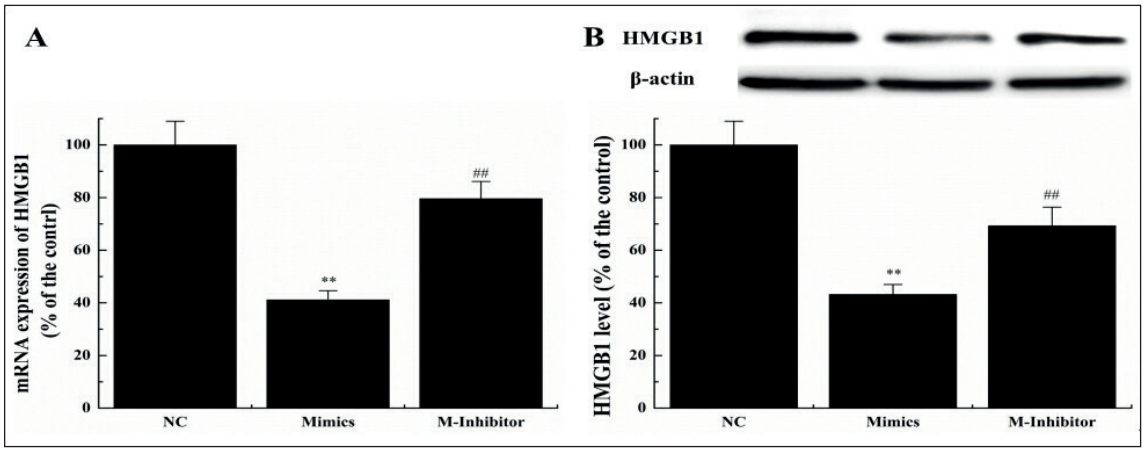

Figure 4. Effect of microRNA-520a-3p on HMGB1 mRNA and protein expression. A, HMGB1 mRNA expression performed by RT-PCR. B, HMGB1 protein expression by Western Blot. The quantitative analysis was carried out by Alpha View SA Software. The data were as mean ± SD. $^{**}p<0.01$, compared with Control group; $^{\#\#}p<0.01$, compared with the Mimics group.

Effect of microRNA-520a-3p on MMP-2/9 Expression in NCI-H157 Tumor Xenograft Growth in Nude Mice

Expression of two HMGB1 associated proteins, MMP-2 and MMP-9, was detected through Western blot (Figure 5A). The results showed that microRNA-520a-3p analog could significantly decreased MMP-2 and MMP-9 expression, which were about 58% and 50%, respectively ($p<0.01$). However, compared with Mimic group, the M-Inhibitors significantly improved expression of MMP-2 and MMP-9 ($p<0.05$). Apoptosis associated proteins, including Bcl-1 and Bax, were also evaluated (Figures 5B and 5C). Mi-

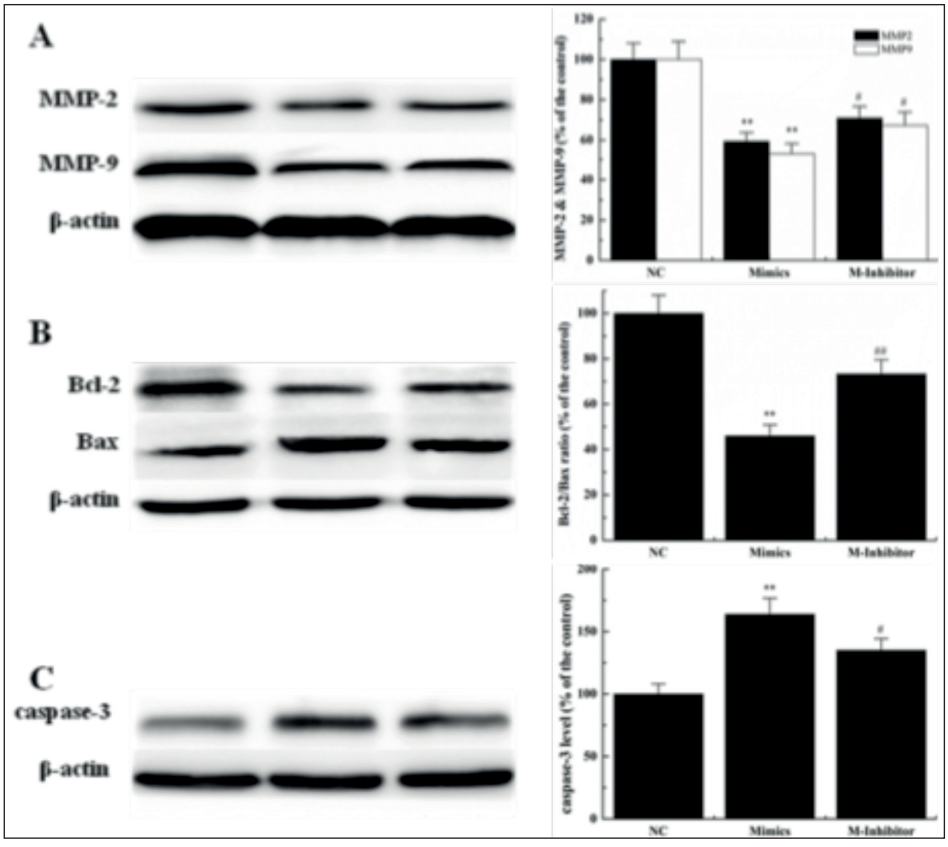

Figure 5. Effect of microRNA-520a-3p on expression of HMGB1 associated proteins. The protein levels of MMP-2/9 (**A**), Bcl-2, Bax (**B**) and caspase 3 (**C**) detected by Western blot. Data are presented as mean ± SD. The quantitative analysis was carried out by Alpha View SA Software. $^{*}p<0.05$; $^{**}p< 0.01$, compared with the Control group; $^{\#}p< 0.05$; $^{\#\#}p< 0.01$, compared with the Mimics group.

croRNA-520-3p apparently exhibited an opposite effect on Bcl-2 and Bax. As shown in Figure 5B, Bcl-2/Bax ratio was significantly decreased compared with Control group ($p<0.01$). After microRNA-520a-3p inhibitor treatment, Bcl-2/Bax ratio was significantly reversed. MicroRNA-520a-3p analog also inhibited the Caspase-3 expression, decreased the cell apoptosis.

Discussion

Non-small-cell lung cancer (NSCLC) is the most common type of lung cancer. As cancer is correlated with epigenetic alterations as well as genetic mutations, a lot of research has been carried out on changes of miRNAs in cancer patients[20]. MicroRNAs are potentially good molecular markers for NSCLC for several main reasons, such as microRNAs are highly specific and relatively stable, and they can be detected in body fluids and easily with non-invasive methods. On the other hand, they might be involved in lung cancer development, epithelial-mesenchymal transition and therapy response. A number of meta-studies have been carried out to identify miRNAs that are potential diagnostic and prognostic markers in cancer; for example, Huang et al[21] analyzed over 3423 healthy and diseased cases from 50 studies, and concluded that miRNAs in circulation, particularly miR-21 and miR-122, may be promising early biomarkers for hepatocellular carcinoma. In case of NSCLC, microRNAs have also been widely reported to be linked to cancer development, epithelial-mesenchymal transition and treatment response. Many miRNAs have been found, including miR-1254 and miR-574-5p[22], miR-328[23], miR-20a, miR-145, miR-21, miR223, and miR-221[24], which were potential early NSCLC markers. Markou et al[8] used liquid bead array technology to study 65 individuals, and confirmed 8 miRNAs, namely miR-21, miR-30d, miR-451, miR-10a, miR-30e-5p, miR-126, miR-126, and miR-145, which were differentially expressed in NSCLC patients and healthy individuals. It has also found that NSCLC patients have significantly elevated levels of miR-499[25]. The large volume of data reflects the high potential of miRNA as a pathological marker for NSCLC, but also warrants further studies and confirmations.

High mobility group box 1 protein (HMGB1) is also called amphoterin, and it is a non-histone key component in the chromatin. It is overexpressed in multiple cancers, and it has been shown to play important roles in tumorigenesis and cancer progression. How it works, however, is not yet clear. HMGB1 has been reported to stimulate tumor cell proliferation by promoting MMP-2, MMP-9, and it has been shown to bind to, and activate, several factors including RAGE-Ras-MAPK, toll-like receptors, NF-kappaB, and Src family kinase signaling pathways[16]. HMGB1 has been reported by Volp et al[26] to be a negative regulator of Caspas-3 and Caspase-9 in human colon carcinomas. On the other hand, a previous report[27] showed that it also regulates tumor-associated cell migration by up-regulating Bcl and down-regulating Bax in carcinoma. Genetic polymorphisms of HMGB1 and HMGB2 have been reported to differential response to platinum-based chemotherapy in both recessive and genotypic models of lung cancer patients[28]. Based on the observational results and proposed signaling mechanisms, HMGB1 was first proposed to be a cancer treatment target in 2013, and a lot of researches have been carried out to assess its effectiveness[13,29]. In relation to NSCLC, the rate of positive HMGB1 expression in the NSCLC tissues has been shown to be significantly higher than in normal tissues, indicating that HMGB1, along with NF-kappaB p65, may be related to non-small cell lung cancer metastasis. Additionally, studies[15,30] have shown that HMGB1 can induce cell motility in NSCLC tumor cells by activating alphavbeta3/FAK through TLR4/NF-kappaB signaling.

In our work, we investigated the effect of microRNA-520-3p analog/inhibitor treatment on the NCI-H157 cells, and studied expression changes in HMGB1 and its downstream proteins. We have found that microRNA-520a-3p suppresses NCI-H157 cell proliferation, migration and invasion, and induces its apoptosis. When transplanted into nude mice, microRNA-520-3p slowed tumor growth down, downregulated the expression of HMGB1 and its effectors, including MMP-2, MMP-9 and Bcl-2, and up-regulated Bax and Caspase-3. The data show that microRNA-520-3p could inhibit NSCLC tumor cell growth, at least partially by suppressing HMGB1.

Conclusions

We showed that microRNA-520a-3p can suppress NCI-H157 cell proliferation, migration and invasion, and induces cell apoptosis. The underlying mechanisms might be partially related to the suppression of HMGB1. Therefore, microRNA-520-3p and HMGB1 may open up new avenues for novel diagnostic and treatment of NSCLC.

Ethical Approval

The research was conducted in accordance with the Declaration of Helsinki and Ethics Committee of Linyi People's Hospital.

Conflict of Interest

The authors declare that there is no conflict of interest.

References

1) Dholaria B, Hammond W, Shreders A, Lou Y. Emerging therapeutic agents for lung cancer. J Hematol Oncol 2016; 9: 138.
2) Travis WD, Brambilla E, Noguchi M, Nicholson AG, Geisinger K, Yatabe Y, Powell CA, Beer D, Riely G, Garg K. International association for the study of lung cancer/american thoracic society/european respiratory society international multidisciplinary classification of lung adenocarcinoma. J Thorac Oncol 2011; 6: 244-285.
3) Klittich WS, Caro DJJ. Lung cancer screening. Am J Respir Med 2002; 1: 393-401.
4) Goldstraw P, Ball D, Jett JR, Le Chevalier T, Lim E, Nicholson AG, Shepherd FA. Non- small-cell lung cancer. Lancet 2011; 378: 1727-1740.
5) Xu FX, Zhang YL, Liu JJ, Zhang DD, Chen HB. Hypoxic markers in non-small cell lung cancer (NSCLC) – a review. Eur Rev Med Pharmacol Sci 2016; 20: 849-852.
6) Hou J, Meng F, Chan LW, Cho WC, Wong SC. Circulating plasma microRNAs as diagnostic markers for NSCLC. Front Genet 2016; 7: 193.
7) Wang H, Wu S, Zhao L, Zhao J, Liu J, Wang Z. Clinical use of microRNAs as potential non-invasive biomarkers for detecting non-small cell lung cancer: a meta-analysis. Respirology 2015; 20: 56-65.
8) Markou A, Sourvinou I, Vorkas PA, Yousef GM, Lianidou E. Clinical evaluation of microRNA expression profiling in non small cell lung cancer. Lung Cancer 2013; 81: 388-396.
9) Kaymaz BT, Cetintas VB, Aktan C, Kosova B. MicroRNA-520a-5p displays a therapeutic effect upon chronic myelogenous leukemia cells by targeting STAT3 and enhances the anticarcinogenic role of capsaicin. Tumour Biol 2014; 35: 8733-8742.
10) Wang X, Wang P, Zhu Y, Zhang Z, Zhang J, Wang H. MicroRNA-520a attenuates proliferation of Raji cells through inhibition of AKT1/NF-kappaB and PERK/eIF2alpha signaling pathway. Oncol Rep 2016; 36: 1702-1708.
11) Yu J, Tan Q, Deng B, Fang C, Qi D, Wang R. The microRNA-520a-3p inhibits proliferation, apoptosis and metastasis by targeting MAP3K2 in non-small cell lung cancer. Am J Cancer Res 2015; 5: 802-811.
12) Hu Q, Zhou Y, Ying K, Ruan W. IGFBP, a novel target of lung cancer? Clin Chim Acta 2017; 466: 172-177.
13) Lotze MT, DeMarco RA. Dealing with death: HMGB1 as a novel target for cancer therapy. Curr Opin Investig Drugs 2003; 4: 1405-1409.
14) Meng Q, Zhao J, Liu H, Zhou G, Zhang W, Xu X, Zheng M. HMGB1 promotes cellular proliferation and invasion, suppresses cellular apoptosis in osteosarcoma. Tumour Biol 2004; 35: 12265-12274.
15) Zhu J, Luo J, Li Y, Jia M, Wang Y, Huang Y, Ke S. HMGB1 induces human non-small cell lung cancer cell motility by activating integrin alphavbeta3/FAK through TLR4/NF-kappaB signaling pathway. Biochem Biophys Res Commun 2016; 480: 522-527.
16) Chen Y, Lin C, Liu Y, Jiang Y. HMGB1 promotes HCC progression partly by downregulating p21 via ERK/c-Myc pathway and upregulating MMP-2. Tumour Biol 2016; 37: 4399-4408.
17) Yao S, Zhao T, Jin H. Expression of microRNA-325-3p and its potential functions by targeting HMGB1 in non-small cell lung cancer. Biomed Pharmacother 2015; 70: 72-79.
18) Zhang C, Ge S, Hu C, Yang N, Zhang J. MiRNA-218, a new regulator of HMGB1, suppresses cell migration and invasion in non-small cell lung cancer. Acta Biochim Biophys Sin 2013; 45: 1055-1061.
19) Qian J, Bai H, Gao Z, Dong YU, Pei J, Ma M, Han B. Downregulation of HIF-1alpha inhibits the proliferation and invasion of non-small cell lung cancer NCI-H157 cells. Oncol Lett 2016; 11: 1738-1744.
20) Del Vescovo V, Denti MA. microRNA and lung cancer. Adv Exp Med Biol 2015; 889: 153-177.
21) Huang JT, Liu SM, Ma H, Yang Y, Zhang X, Sun H, Zhang X, Xu J, Wang J. Systematic review and meta-analysis: circulating miRNAs for diagnosis of hepatocellular carcinoma. J Cell Physiol 2016; 231: 328-335.
22) Foss KM, Sima C, Ugolini D, Neri M, Allen KE, Weiss GJ. miR-1254 and miR-574-5p: serum-based microRNA biomarkers for early-stage non-small cell lung cancer. J Thorac Oncol 2011; 6: 482-488.
23) Ulivi P, Foschi G, Mengozzi M, Scarpi E, Silvestrini R, Amadori D, Zoli W. Peripheral blood miR-328 expression as a potential biomarker for the early diagnosis of NSCLC. Int J Mol Sci 2013; 14: 10332-10342.
24) Geng Q, Fan T, Zhang B, Wang W, Xu Y, Hu H. Five microRNAs in plasma as novel biomarkers for screening of early-stage non-small cell lung cancer. Respir Res 2014; 15: 149.
25) Li M, Zhang Q, Wu L, Jia C, Shi F, Li S, Peng A, Zhang G, Song X, Wang C. Serum miR-499 as a novel diagnostic and prognostic biomarker in non-small cell lung cancer. Oncol Rep 2014; 31: 1961-1967.
26) Völp K, Brezniceanu ML, Bösser S, Brabletz T, Kirchner T, Göttel D, Joos S, Zörnig M. Increased expression of high mobility group box 1 (HMGB1) is associated with an elevated level of the antiapop-

totic c-IAP2 protein in human colon carcinomas. Gut 2006; 55: 234-242.

27) Ko YB, Kim BR, Nam SL, Yang JB, Park SY, Rho SB. High-mobility group box 1 (HMGB1) protein regulates tumor-associated cell migration through the interaction with BTB domain. Cell Signal 2014; 26: 777-783.

28) Wang Y, Li XP, Yin JY, Zhang Y, He H, Qian CY, Chen J, Zheng Y, Smieszkol K, Fu YL, Chen ZY, Zhou HH, Liu ZQ. Association of HMGB1 and HMGB2 genetic polymorphisms with lung cancer chemotherapy response. Clin Exp Pharmacol Physiol 2014; 41: 408-415.

29) Ju LL, Zhao CY, Ye KF, Yang H, Zhang J. Expression and clinical implication of Beclin1, HMGB1, p62, survivin, BRCA1 and ERCC1 in epithelial ovarian tumor tissues. Eur Rev Med Pharmacol Sci 2016; 20: 1993-2003.

30) Zhang X, Wang H, Wang J. Expression of HMGB1 and NF-kappaB p65 and its significance in non-small cell lung cancer. Contemp Oncol (Pozn) 2013; 17: 350-355.